

---

This is an electronic reprint of the original article.

This reprint may differ from the original in pagination and typographic detail.

González Escobedo, José Luis; Mäkelä, Eveliina; Neuvonen, Jouni; Uusi-Kyyny, Petri; Lindblad, Marina; Karinen, Reetta; Puurunen, Riikka L.

**Hydrodeoxygenation of Propylphenols on a Niobia-Supported Platinum Catalyst : Ortho, Meta, Para Isomerism, Reaction Conditions, and Phase Equilibria**

*Published in:*  
Advanced Sustainable Systems

*DOI:*  
[10.1002/adsu.201900140](https://doi.org/10.1002/adsu.201900140)

Published: 01/10/2020

*Document Version*  
Publisher's PDF, also known as Version of record

*Published under the following license:*  
CC BY-NC-ND

*Please cite the original version:*  
González Escobedo, J. L., Mäkelä, E., Neuvonen, J., Uusi-Kyyny, P., Lindblad, M., Karinen, R., & Puurunen, R. L. (2020). Hydrodeoxygenation of Propylphenols on a Niobia-Supported Platinum Catalyst : Ortho, Meta, Para Isomerism, Reaction Conditions, and Phase Equilibria. *Advanced Sustainable Systems*, 4(10), Article 1900140. <https://doi.org/10.1002/adsu.201900140>

# Hydrodeoxygenation of Propylphenols on a Niobia-Supported Platinum Catalyst: *Ortho*, *Meta*, *Para* Isomerism, Reaction Conditions, and Phase Equilibria

José Luis González Escobedo,\* Eveliina Mäkelä, Jouni Neuvonen, Petri Uusi-Kyyny, Marina Lindblad, Reetta Karinen, and Riikka L. Puurunen

The alkylphenols found in liquefied lignocellulose could become a source of bio-based aromatic hydrocarbons for fuel components. In the hydrodeoxygenation (HDO) of alkylphenols, hydroxyl groups must be removed while avoiding the hydrogenation of the aromatic ring. Here, the HDO of propylphenols is studied using a Pt/Nb<sub>2</sub>O<sub>5</sub> catalyst and *n*-tetradecane solvent. HDO experiments are performed using different reaction conditions of batch residence time (0–161 min  $g_{cat} g_{reactant}^{-1}$ ), pressure (20–30 bar H<sub>2</sub>), and temperature (300–375 °C). HDO is studied with *ortho*-, *meta*-, and *para*-propylphenol. The influence of vapor–liquid equilibrium and chemical equilibrium are assessed using thermodynamic calculations. Almost full deoxygenation is attained in the experiments; the main products are propylbenzene and propylcyclohexane. The study finds that, of the isomers, 4-propylphenol is the most favorable for forming propylbenzene (77% maximum selectivity), whereas 2-propylphenol is the least favorable (55% maximum selectivity). Additionally, the reactivity of propylbenzene in the test conditions is detrimental to its selectivity after 5 min  $g_{cat} g_{reactant}^{-1}$ . Finally, the temperature at which the process favors propylbenzene is found to shift as a function of pressure; at 20 bar, propylbenzene is favored at 350 °C and at 30 bar, it is favored at 375 °C.

managed responsibly.<sup>[2,3]</sup> Such renewable biofuels are especially promising for sustainable aviation.<sup>[4]</sup> The biopolymers that constitute lignocellulose can be broken down, among other means, by liquefaction.<sup>[5–7]</sup> Liquefaction relies on thermochemistry (200–400 °C) and on a liquid solvent, such as a high boiling point hydrocarbon.<sup>[6,7]</sup> The same solvent can be used in subsequent upgrading steps. The product of liquefaction is biocrude: a complex mixture of phenolics, furanics, cyclic ketones, carboxylic acids, and other compounds.<sup>[6]</sup> The high concentration of oxygenates renders biocrudes chemically unstable, poor in heating value, corrosive, highly viscous, and prone to form coke.<sup>[6,8]</sup> Hence, further upgrading is necessary, with a possible upgrading step being hydrodeoxygenation (HDO): a type of hydrotreatment, in which biocrude constituents react with dihydrogen on a heterogeneous catalyst, producing deoxygenated compounds and water.<sup>[8]</sup> Fittingly,

HDO can proceed in the presence of an organic solvent.<sup>[7]</sup>

Liquefaction biocrudes are highly unsaturated (60–65% carbon) and resemble lignin or pyrolysis liquids.<sup>[6]</sup> They are rich in phenolic compounds, and hence they are a potential source of bio-based aromatic hydrocarbons. Aromatic hydrocarbons are essential to the chemical industry,<sup>[9–12]</sup> and they are also required in fuels.<sup>[4]</sup> For example, international standards stipulate that jet fuel should contain 8% to 25% aromatics.<sup>[4,13,14]</sup> Although the abundant phenolics produced in liquefaction are suitable for conversion to aromatic hydrocarbons via HDO, the challenge, especially with alkylphenols, is that the aryl-hydroxyl bond is among the strongest in lignocellulose.<sup>[8]</sup> Furthermore, it is necessary to prevent the hydrogenation of the aromatic ring. Thus, in order to overcome these obstacles, it is pertinent to study the HDO of alkylphenols, for which catalyst development is essential. Many factors in the HDO process can influence the performance of a HDO catalyst. Some of these factors are the reaction medium,<sup>[15,16]</sup> the reaction temperature and pressure with their thermodynamic and kinetic effects,<sup>[17]</sup> and the *ortho*, *meta*, and *para* isomerism of alkylphenols.<sup>[18]</sup>

Sulfided catalysts are considered conventional in commercial hydrotreatment.<sup>[19,20]</sup> Unfortunately, the activity of sulfided


## 1. Introduction

Lignocellulose is an abundant renewable resource,<sup>[1]</sup> which can be used sustainably to produce transportation biofuels, when

J. L. González Escobedo, E. Mäkelä, J. Neuvonen, Dr. P. Uusi-Kyyny, Dr. R. Karinen, Prof. R. L. Puurunen

Aalto University  
Department of Chemical and Metallurgical Engineering  
P.O. Box 16100, Aalto 00076, Finland  
E-mail: jose.gonzalezescobedo@aalto.fi

Dr. M. Lindblad  
Neste Corporation  
P.O. Box 310, Porvoo 06101, Finland

 The ORCID identification number(s) for the author(s) of this article can be found under <https://doi.org/10.1002/adsu.201900140>.

© 2020 The Authors. Published by WILEY-VCH Verlag GmbH & Co. KGaA, Weinheim. This is an open access article under the terms of the Creative Commons Attribution-NonCommercial-NoDerivs License, which permits use and distribution in any medium, provided the original work is properly cited, the use is non-commercial and no modifications or adaptations are made.

DOI: 10.1002/adsu.201900140

catalysts can only be maintained by continuously feeding a sulfiding agent during operation.<sup>[20,21]</sup> Hence, it is important to develop catalysts that can retain their activity independently. Platinum has been found to be effective in the hydrotreatment of alkylphenols.<sup>[22–26]</sup> Aromatic products can be formed on Pt,<sup>[27]</sup> especially on bifunctional Pt catalysts.<sup>[23,28–30]</sup> Noronha, Resasco and co-workers<sup>[29,31–33]</sup> have studied alkylphenol HDO with a bifunctional, niobia-supported palladium catalyst. Niobia, a reducible oxide,<sup>[34]</sup> is a promising support for bifunctional catalysts:<sup>[32,33,35]</sup> compared to Pd/SiO<sub>2</sub>, Pd/Nb<sub>2</sub>O<sub>5</sub> provided a 40-fold higher selectivity to benzene in phenol HDO.<sup>[32]</sup> A similar catalyst, multifunctional Pt/NbOPO<sub>4</sub>, has been used in the one-pot conversion of wood sawdust into hexane, pentane, and alkylcyclohexanes with yields up to 28.1 wt%.<sup>[36]</sup> Nevertheless, niobia has been studied rarely in the HDO literature. To our knowledge, no studies on the HDO of alkylphenols to produce aromatics have been reported with a Pt/Nb<sub>2</sub>O<sub>5</sub> catalyst, which was chosen for this study.

Regarding the reaction medium in alkylphenol HDO, recent studies have focused on vapor-phase operation, and they often report high selectivities to aromatic hydrocarbons.<sup>[23,31–33,37]</sup> However, HDO in liquid solvents might be beneficial for integration with liquefaction. Many studies on the HDO of phenolics with solvents have focused mostly on guaiacol, rather than on alkylphenols. Hellinger et al.<sup>[15]</sup> studied the performance of Pt catalysts in guaiacol HDO with various solvents. They observed that hydrocarbon solvents led to better conversions and degrees of deoxygenation, while simultaneously causing less Pt sintering than oxygenated solvents or the solvent-free operation. The solvent can influence the HDO of phenolics through the solubility of H<sub>2</sub>, the solvent-catalyst interactions, and the solvent-reactant interactions.<sup>[16]</sup> A high solubility of H<sub>2</sub> in the solvent has been connected with full ring hydrogenation.<sup>[26]</sup> However, He et al.<sup>[16]</sup> observed that, although the solubility of H<sub>2</sub> is higher in *n*-hexadecane than in methanol or water, the rate of phenol hydrogenation on Pt catalysts was lower with the alkane solvent than with the polar solvents. The high interaction of *n*-hexadecane with the catalysts was proposed to restrict phenol hydrogenation.<sup>[16]</sup> Furthermore, hydrocarbon solvents have been observed to enhance the adsorption of a polar compound, cyclohexanone, and hinder the adsorption of a non-polar compound, cyclohexane.<sup>[38]</sup> Thus, perhaps, hydrocarbon solvents might also enhance the adsorption of phenols and hinder the adsorption of alkyl benzenes. However, Nelson et al.<sup>[39]</sup> suggested that non-polar solvents such as *n*-octane occlude the active sites of oxide-supported noble metal catalysts in the HDO of phenols. In view of the possible benefits of using alkane solvents, *n*-tetradecane was selected for this study and compared with *n*-octane to account for possible drawbacks.

When performing three-phase HDO with liquid solvents, it is important to consider the effect of the reaction conditions on the phase behavior of the reaction mixture. Turpeinen et al.<sup>[40]</sup> argued that the most suitable approach to model vapor–liquid equilibrium (VLE) in HDO is to apply equations of state (EoS) combined with predictive activity coefficient models (PAC). HDO always involves supercritical H<sub>2</sub> (critical temperature 32.938 K<sup>[41]</sup>), such that PACs per se do not apply, and simultaneously, the interactions of the many components in HDO require predictive modeling, which pure EoSs lack. The Predictive Soave–Redlich–Kwong (PSRK)<sup>[42]</sup> method was found effective for HDO in a liquid organic medium,<sup>[40]</sup> hence it was applied in this work to study the phase behavior of the reaction mixture.

Concerning the reaction conditions, it has been observed that hydrogenated products are favored at low temperatures, whereas aromatics are formed at high temperatures.<sup>[17,43]</sup> Zhang et al.<sup>[44]</sup> tested phenol HDO on MoO<sub>3</sub> at 0.5 atm H<sub>2</sub> and 0.5 atm N<sub>2</sub>. They noticed an increase in benzene selectivity from 73.9% at 300 °C to 97.2% at 400 °C. Similarly, Barrios et al.<sup>[32]</sup> tested phenol HDO on Pd/Nb<sub>2</sub>O<sub>5</sub> at 1 atm H<sub>2</sub> and observed that, by increasing the temperature from 200 to 400 °C, benzene selectivity rose from 13.8% to 99.6% and conversion, from 6.4% to 10.1%. Griffin et al.<sup>[23]</sup> studied the combined effect of temperature and pressure on *m*-cresol HDO on Pt/TiO<sub>2</sub>. At 250 °C and 20 bar, the sum of the selectivities of C<sub>6</sub> oxygenates was 95%. By contrast, at 350 °C and 5 bar, the oxygenate selectivity was only 17%, and methylbenzene selectivity was 78%.

In this work, we present the conditions at which propylbenzene was obtained with a high selectivity from 4-propylphenol in *n*-tetradecane solvent and with a 3.1% Pt/Nb<sub>2</sub>O<sub>5</sub> catalyst. The main byproduct was propylcyclohexane, and nearly full deoxygenation was attained. The aim of this work, aside of obtaining a high propylbenzene selectivity, was to determine the influence of various process parameters on the performance of the catalyst. Thus, we studied the *ortho*, *meta*, *para* isomerism, the H<sub>2</sub> pressure, and the temperature. Furthermore, we discussed the influence of VLE and of chemical equilibrium on the results.

## 2. Results and Discussion

### 2.1. Catalyst Characterization

According to XRF, the metal loading of the Pt/Nb<sub>2</sub>O<sub>5</sub> catalyst was 3.1%. The textural characteristics of the catalyst and the support, which were obtained from physisorption, chemisorption, and STEM images, are reported in Table 1. The physisorption

**Table 1.** Textural characteristics of the Pt/Nb<sub>2</sub>O<sub>5</sub> and the plain support.

Catalyst	$S_{\text{BET}}$ [m <sup>2</sup> g <sup>−1</sup> ] <sup>a)</sup>	Pore volume [cm <sup>3</sup> g <sup>−1</sup> ] <sup>b)</sup>	Pore diameter average [nm] <sup>b)</sup>	Pore diameter mode [nm] <sup>b)</sup>	Metal dispersion <sup>c)</sup>	Chemisorption average particle size [nm] <sup>c)</sup>	STEM average particle size [nm] <sup>d)</sup>
Nb <sub>2</sub> O <sub>5</sub>	74	0.12	6.9	6.2	—	—	—
3.1% Pt/Nb <sub>2</sub> O <sub>5</sub> <sup>e)</sup>	85	0.10	5.3	4.5	41%	2.5	1.4

<sup>a)</sup>Calculated with the BET method from N<sub>2</sub> physisorption, 0.05–0.3 *p/p*<sup>0</sup>; <sup>b)</sup>Calculated with the BJH method from N<sub>2</sub> physisorption, 0.2–0.9 *p/p*<sup>0</sup>; <sup>c)</sup>From CO chemisorption at 25 °C, performed after sample reduction at 290 °C. The irreversible CO adsorption capacity was 63.4 μmol g<sub>cat</sub><sup>−1</sup>; <sup>d)</sup>From 196 measurements; standard deviation: 0.3 nm; <sup>e)</sup>Metal loading from XRF.

**Table 2.** Summary of control experiments.

Experiment <sup>a)</sup>	Reactant	Catalyst	Reaction time [min] <sup>b)</sup>	Key results <sup>c)</sup>
Blank 1	none	Pt/Nb <sub>2</sub> O <sub>5</sub>	35	Negligible solvent conversion
Blank 2	4-propylphenol	none	60	16.3% loss of reactant in decomposition and evaporation
Cooling experiment	4-propylphenol	Pt/Nb <sub>2</sub> O <sub>5</sub>	0	Reactor cooling influences conversion results, but not product distributions
Experiment with bare support	4-propylphenol	Nb <sub>2</sub> O <sub>5</sub>	35	43% conversion and 34% selectivity to aromatic ether

<sup>a)</sup>The experiment parameters were: 20 bar H<sub>2</sub>, 350 °C, ≈65 mg catalyst (where applicable), ≈580 mg reactant (where applicable), and 20.5 g C<sub>14</sub>H<sub>30</sub> solvent; <sup>b)</sup>The reaction time is the time that the reactor spent at reaction temperature; <sup>c)</sup>More details on Tables S1 and S3 (Supporting Information).

isotherms of the catalyst and the support presented a double hysteresis loop (Figure S1a, Supporting Information). Pore size distributions were calculated from the physisorption isotherms (Figure S1b, Supporting Information). The CO chemisorption isotherms are presented in Figure S1c (Supporting Information), and the histogram of the particles measured on the STEM images is presented in Figure S1d (Supporting Information). A selection of STEM images is presented in Figure S2 (Supporting Information).

Pt appeared to be well dispersed on the niobia support. The differences in particle size obtained from chemisorption (2.5 nm) and STEM (1.4 nm) can be partly explained by the pretreatment (reduction) that preceded chemisorption but not STEM. The difference is greater than three standard deviations of the sample of particles measured on the STEM images. The high dispersion might be one of the factors that enabled the high activity of the catalyst (Section 2.3).

## 2.2. Control Experiments

Experiments and calculations were performed to account for the sources of uncertainty in HDO experiments. From blank experiments, which are discussed in Section S4.1 (Supporting Information) and summarized in Table 2, it can be concluded that the reactivity of the solvent was negligible with the catalyst at 350 °C and 20 bar H<sub>2</sub>. Furthermore, evaporation and loss of reactant and products, evident in the carbon balances and  $\Sigma Sm$  (Equation (5) and Table S3, Supporting Information), introduced uncertainties to the determination of final reactant and product amounts. The uncertainties in the product distributions are less than in the yields, product amounts, and selectivities. 4-Propylphenol likely underwent thermal reactions to a lesser degree than it was lost in evaporation. The cooling after the experiments (Section S4.2, Supporting Information) introduced uncertainties to the conversions. However, the effect of cooling on product selectivities was minor. The external and internal mass transfer limitations (Sections S4.3 and S4.4, Supporting Information) were negligible. Finally, repeated experiments at 3.9 and 5.1 min g<sub>cat</sub> g<sub>reactant</sub><sup>-1</sup> (Figure 1) reported a negligible variation in conversion and a variation of 10% points in propylbenzene selectivity and 12% points in propylcyclohexane selectivity.

The niobia support was active without platinum. After reducing the support at 20 bar and 353 °C for 60 min, a HDO experiment at 20 bar, 350 °C, and  $\tau_B = 3.9$  min mg<sub>cat</sub> mg<sub>reactant</sub><sup>-1</sup> resulted in a conversion of 43%. The amounts of propylbenzene and propylcyclohexane were negligible. 4-Propylcyclohexanol,

phenol, methylbenzene, and gases were formed with selectivities of 11%, 3.4%, 2.6%, and 2.7%, respectively. By contrast, the highest selectivity, 34%, was to a compound identified with GC-MS electron ionization and GC-MS chemical ionization (Figure S3, Supporting Information) as an aromatic ether, 1-methoxy-4-(1-methylpropyl)-benzene; the NIST match factor was >900. This compound was not found in the fresh reactant, although it was formed in the blank experiment without catalyst. The formation of the aromatic ether is surprising, as O-alkylation often occurs in presence of highly acidic or basic catalysts.<sup>[45]</sup> It is known that phenol can decompose spontaneously through a radical mechanism in the gas phase.<sup>[46]</sup> Phenol breaks down to CO and cyclopentadiene, which in turn forms acetylene and propargyl radical.<sup>[46]</sup> Both CO and acetylene were detected in the blank experiment (Section S4.1, Supporting Information). Hence, the compound identified in this work as an aromatic ether might have been formed in the gas phase by reaction of 4-propylphenol with radicals formed by the decomposition of other 4-propylphenol molecules.

An experiment with Pt/Nb<sub>2</sub>O<sub>5</sub> was performed using *n*-octane as a solvent for comparison with *n*-tetradecane. The reaction conditions were 20 bar H<sub>2</sub>, 350 °C, and  $\tau_B = 0.2$  min g<sub>cat</sub> g<sub>reactant</sub><sup>-1</sup>. The 4-propylphenol conversion with *n*-octane solvent was 13%, whereas at equal conditions, it was 44% with *n*-tetradecane solvent (Figure S7, Supporting Information). Furthermore, with *n*-octane, the yields of propylbenzene and propylcyclohexane were negligible and the yield of 1-methoxy-4-(1-methylpropyl)-benzene, the main liquid product, was 3%. The possible poisoning of the catalyst by S contaminants in *n*-octane was discarded, as S in both solvents was below the detection limit of the ASTM method. Nelson et al.<sup>[39]</sup> suggested that *n*-octane

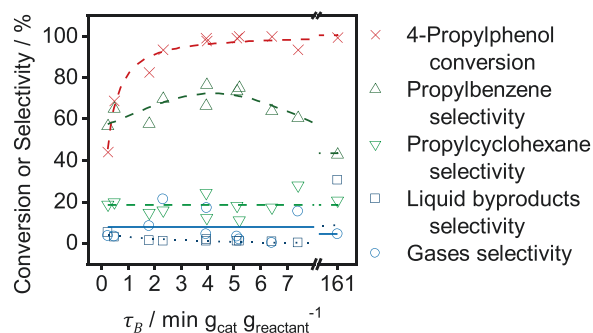


**Figure 1.** 4-Propylphenol conversion and product selectivity in HDO with respect to batch residence time ( $\tau_B$ ). Experiment parameters: 3.1%Pt/Nb<sub>2</sub>O<sub>5</sub> catalyst, 20 bar H<sub>2</sub>, 350 °C, 580 mg reactant, 20.5 g C<sub>14</sub>H<sub>30</sub> solvent. The lines are included to guide the eye. Note the scale break.

can occlude the active sites of the catalysts at 300 °C. It must be noted that *n*-octane was supercritical at the tested conditions (critical temperature, 259 °C<sup>[41]</sup>). Furthermore, according to the PSRK model (Section 2.5), 4-propylphenol (critical temperature, 464 °C<sup>[41]</sup>) resided completely in the vapor phase at the tested conditions with *n*-octane. Thus, as the reaction system with *n*-octane contained only two phases instead of three, the fraction of H<sub>2</sub> in the reaction mixture was not limited by its solubility; therefore, a higher HDO rate would be expected. As the opposite was the case, *n*-octane might have hindered the reaction, although the specific mechanism remains unclear.

### 2.3. Activity and Selectivity with 4-Propylphenol

A series of HDO experiments with 4-propylphenol was conducted at consecutive batch residence times ( $\tau_B$ , min  $g_{cat} g_{reactant}^{-1}$ ). The results of this series of experiments are presented in Figure 1 and Table S1 (Supporting Information). The catalyst had an initial turnover frequency (TOF) of 4.1 s<sup>-1</sup>. The highest selectivity to propylbenzene was 77% at 3.9 min  $g_{cat} g_{reactant}^{-1}$ . Up to 8 min  $g_{cat} g_{reactant}^{-1}$ , the 4-propylphenol conversions ranged from 44% to 100%, while the selectivities to propylbenzene and propylcyclohexane remained on average at 67% (standard deviation 1s = 7%, from all the selectivity data points between 0 and 8 min  $g_{cat} g_{reactant}^{-1}$ ) and 18% (1s = 5%), respectively. However, propylbenzene selectivity increased slightly from 0.25 to 5 min  $g_{cat} g_{reactant}^{-1}$  and declined slowly afterward. After extending the batch residence time to 161 min  $g_{cat} g_{reactant}^{-1}$  (24 h), the selectivity to propylbenzene dropped to 43%, whereas the selectivity to propylcyclohexane remained within 1s of the previously observed mean. The H<sub>2</sub> conversion in the first experiment was 70%, and at full 4-propylphenol conversion, H<sub>2</sub> conversion settled at 18% on average.

The propylbenzene selectivity reported in this work is comparable to some of the highest in the literature.<sup>[23,25,32,44,47,48]</sup> Whereas oxygenates are among the major products in other works,<sup>[16,23,25]</sup> here mostly hydrocarbons were obtained. Barrios et al.<sup>[32]</sup> found that the selectivity to oxygenates on Pd catalysts was substantially less with Nb<sub>2</sub>O<sub>5</sub> support than with SiO<sub>2</sub>, Al<sub>2</sub>O<sub>3</sub>, TiO<sub>2</sub>, ZrO<sub>2</sub>, and CeO<sub>2</sub>. Comparing to the experiment

with bare Nb<sub>2</sub>O<sub>5</sub> (Section 2.2), Pt was apparently responsible for the hydrogenation and deoxygenation observed with Pt/Nb<sub>2</sub>O<sub>5</sub>. Nevertheless, according to theoretical studies,<sup>[27]</sup> direct deoxygenation is strongly disfavored on Pt, whereas ring hydrogenation is preferred, and oxygenates are also favored. Thus, the preference for propylbenzene observed in this work must be due to a combination of factors, including the Pt-support interaction<sup>[23]</sup> and other process conditions (Sections 2.5 and 2.6). This article focuses on the process conditions.

The combined selectivity to liquid byproducts, aside of propylcyclohexane, was <5.5% at  $\tau_B < 8$  min  $g_{cat} g_{reactant}^{-1}$ . At 161 min  $g_{cat} g_{reactant}^{-1}$ , the selectivity of the liquid byproducts was 30%. The most common liquid byproduct, aside of propylcyclohexane, was methylbenzene. 4-Propylcyclohexanone, 4-propylcyclohexanol, and 1-methoxy-4-(1-methylpropyl)-benzene were formed at  $\tau_B < 2.3$  min  $g_{cat} g_{reactant}^{-1}$  and disappeared afterward, although 4-propylcyclohexanol was also found after the 161 min  $g_{cat} g_{reactant}^{-1}$  experiment. The other liquid byproducts could be classified as in Figure 2 and are listed in Table S2 (Supporting Information). The combined selectivity to gases varied between 3% and 20%. Throughout the residence time series, 46% to 80% of the gases were ethane and 16% to 25% were methane.

In order to assess whether an equilibrium composition was attained, the product distributions of 4-propylphenol HDO at 5 and 161 min  $g_{cat} g_{reactant}^{-1}$  were compared (Figure 2). While the proportion of propylbenzene declined, methyl- and ethylbenzene, C<sub>9</sub> alkylcyclopentanes, C<sub>6</sub> to C<sub>11</sub> alkylcyclohexanes, and naphthalenes were formed. By contrast, the proportion of propylcyclohexane and gases did not change. Furthermore, the hydrotreatment of propylbenzene and propylcyclohexane was tested under the same conditions as 4-propylphenol (Figure 2). After 5 min  $g_{cat} g_{reactant}^{-1}$ , the conversions of propylbenzene and propylcyclohexane were 30% and 18%, respectively. The hydrotreatment of propylbenzene formed mostly propylcyclohexane (50% selectivity) and gases (11% selectivity), while the hydrotreatment of propylcyclohexane formed mostly propylbenzene (59% selectivity) and gases (48% selectivity). Propylcyclohexane dehydrogenation occurred to some degree. The final compositions in propylbenzene hydrotreatment and 4-propylphenol HDO were remarkably similar at 5 min  $g_{cat} g_{reactant}^{-1}$ .

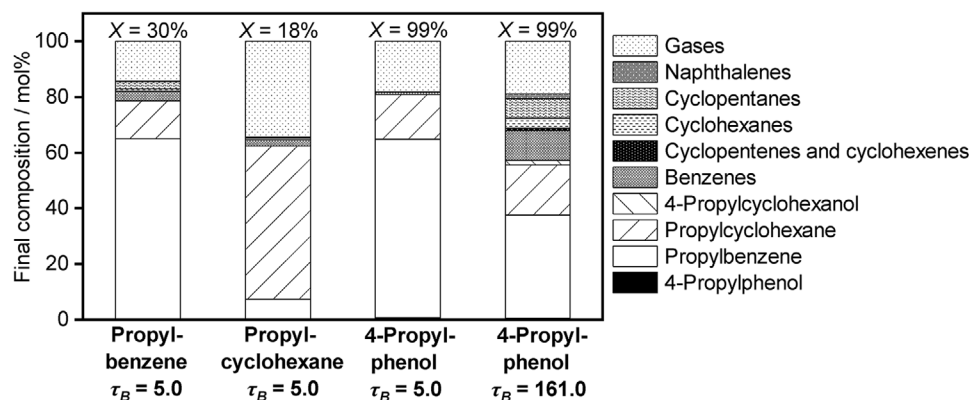


**Figure 2.** Conversions (X) and final molar compositions of reaction mixtures in hydrotreatment of propylbenzene, propylcyclohexane, and 4-propylphenol after the given batch residence times ( $\tau_B$ , min  $g_{cat} g_{reactant}^{-1}$ ). Note that the compositions include the unconverted reactant and exclude the solvent. Experiment parameters: 3.1%Pt/Nb<sub>2</sub>O<sub>5</sub> catalyst, 20 bar H<sub>2</sub>, 350 °C, 580 mg reactant, 20.5 g C<sub>14</sub>H<sub>30</sub> solvent.



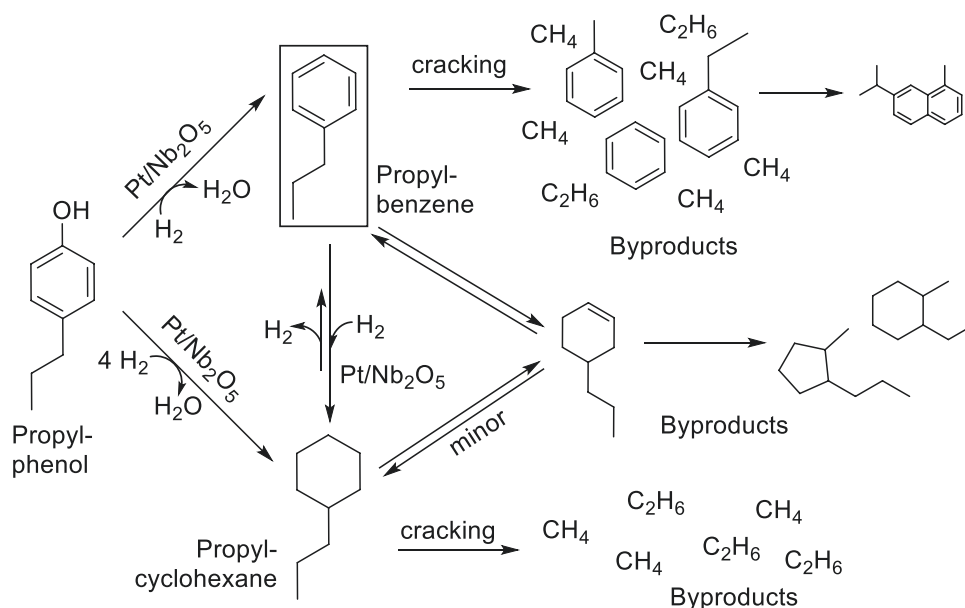
As propylbenzene was reactive with the catalyst and conditions used (Figure 2), propylbenzene likely reacted after being formed, causing its selectivity to drop after attaining a maximum (Figure 1). Propylcyclohexane was less reactive than propylbenzene, thus its selectivity remained roughly unchanged. The lower reactivity of propylbenzene and propylcyclohexane compared to 4-propylphenol can be explained by thermodynamic limitations (Section 2.6 and Figure S11, Supporting Information). In the methylbenzene hydrogenation literature, it has been noted<sup>[49–51]</sup> that full hydrogenation is unfavorable above 200 °C, due to the decrease in catalyst H coverage above that temperature. As for the dehydrogenation of cyclohexanes, it is favored on Pt catalysts, in atmospheric pressure, and at temperatures above 300 °C.<sup>[52–55]</sup> Thus, the low propylcyclohexane dehydrogenation observed in this work was likely due to the high H<sub>2</sub> pressure used in the experiment. The observed deoxygenated byproducts can be explained as being formed mostly from propylbenzene. Methyl- and ethylbenzene likely resulted from the cracking of the propyl sidechain. Cyclopentanes likely formed by the isomerization and ring contraction of the deoxygenated products.<sup>[56,57]</sup> In the present study, unsaturation was apparently necessary for forming cyclopentanes; cyclopentanes were hardly formed from propylcyclohexane (Figure 2). Indeed, according to some authors,<sup>[56,58]</sup> cyclopentanes are formed from cyclohexenes. Naphthalenes were probably formed eventually by the condensation of aromatic products. The gases were formed partly by side-chain cracking and partly by ring opening and cracking, as their amounts exceed the methyl- and ethylbenzene amounts. **Scheme 1** illustrates the results of 4-propylphenol HDO presented in this section.

#### 2.4. Activity and Selectivity with Different Isomers

Aside of 4-propylphenol, HDO on the 3.1% Pt/Nb<sub>2</sub>O<sub>5</sub> catalyst was tested with 2- and 3-propylphenols. A series of experiments

at different residence times was performed in order to compare the results both at low and high conversion. The results with the *ortho* and *meta* isomers are presented in **Figure 3** along with a selection of experiments with the *para* isomer. The differences observed in the conversions and selectivities obtained from the three isomers were greater than the experimental uncertainty (Section 2.2). Initial TOFs were calculated with the data in Figure 3 as 4.9 s<sup>−1</sup> for 2-propylphenol, 1.3 s<sup>−1</sup> for 3-propylphenol, and 4.1 s<sup>−1</sup> for 4-propylphenol. At ≈4 min g<sub>cat</sub> g<sub>reactant</sub><sup>−1</sup>, the conversion was nearly full with the three isomers. The propylbenzene selectivity plateaued at ≈55% with the *ortho* isomer and at ≈62% with the *meta* isomer, whereas it reached 77% with the *para* isomer. Although the selectivity to propylcyclohexane was in all cases lower than to propylbenzene, it was the lowest with the *para* isomer and the highest with the *ortho* isomer. Between 0.5 and 5 min g<sub>cat</sub> g<sub>reactant</sub><sup>−1</sup>, the selectivity to oxygenated byproducts declined from 2.4% to 0.9% with the *para* isomer and from 1.1% to 0.6% with the *ortho* isomer. With the *meta* isomer, oxygenated byproducts were not detected. With the three isomers, the main gases were ethane and methane.

The effect of thermodynamic limitations on the different results observed with the propylphenol isomers could not be determined; the thermodynamic properties found in the literature<sup>[41]</sup> (Table S4, Supporting Information) were calculated with Joback's method, which does not account for isomerism.<sup>[59]</sup> Some authors<sup>[18,60,61]</sup> have observed that *ortho* alkyl phenols are less reactive than unsubstituted phenol. Massoth et al.<sup>[18]</sup> found that *ortho*-methylphenol was less reactive than its *meta* and *para* isomers and that aromatic selectivity was the greatest with the *para* isomer. By contrast, in the present study, the *meta* isomer was the least reactive, although the *para* isomer resulted in the highest aromatic selectivity. Massoth et al.<sup>[18]</sup> demonstrated that the different selectivities observed with the different isomers were due to electrostatic and orbital effects, rather than due to steric effects.



**Scheme 1.** Summary of 4-propylphenol HDO and hydrotreatment of the main HDO products, propylbenzene and propylcyclohexane, on Pt/Nb<sub>2</sub>O<sub>5</sub> catalyst.

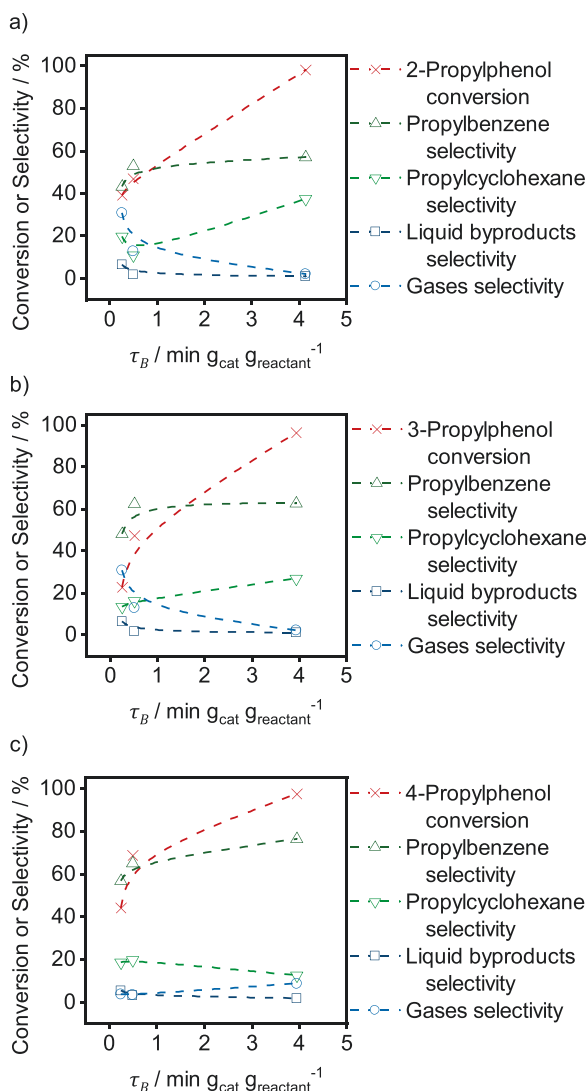


**Figure 3.** Conversions and product selectivities with respect to batch residence time ( $\tau_B$ ) in HDO of a) 2-propylphenol, b) 3-propylphenol, and c) 4-propylphenol. Experiment parameters: 3.1%Pt/Nb<sub>2</sub>O<sub>5</sub> catalyst, 20 bar H<sub>2</sub>, 350 °C, 580 mg reactant, 20.5 g C<sub>14</sub>H<sub>30</sub> solvent. The lines are included to guide the eye.

## 2.5. Effects of Vapor–Liquid Equilibrium

The study of the effects of pressure and temperature in HDO required accounting for the VLE. Because of the small amount of reactant used, the possibility of evaporation was a serious concern, as it is reasonable to assume that the reactions occurred mainly in the liquid phase; most of the catalyst was likely immersed during the experiments. For this reason, a series of VLE calculations for a mixture of 4-propylphenol, H<sub>2</sub>, and C<sub>14</sub>H<sub>30</sub> were performed with the PSRK method for a series of pressures (20 to 80 bar) and temperatures (300 to 375 °C). The results are presented in Figure S8 (Supporting Information). According to the model, at 350 °C and 20 bar H<sub>2</sub>, 67% of the mass of propylphenol and 10% of the mass of H<sub>2</sub> reside in the liquid phase. These proportions correspond to 0.16 mmol propylphenol per gram of liquid solution and 0.23 mmol H<sub>2</sub> g<sup>-1</sup>

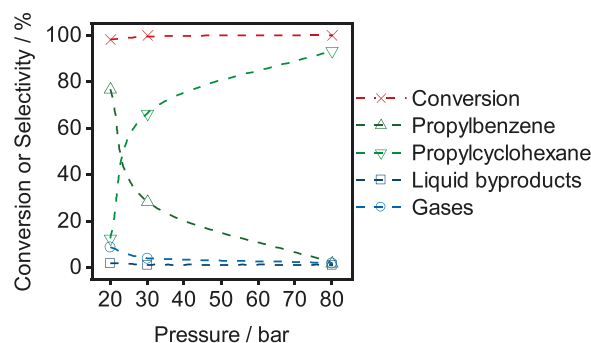


**Figure 4.** Effect of H<sub>2</sub> pressure on product distribution at full conversion of 4-propylphenol. Note that H<sub>2</sub> pressure corresponded to absolute pressure in the experiments. Experiment parameters: 3.1%Pt/Nb<sub>2</sub>O<sub>5</sub> catalyst, 350 °C,  $\tau_B = 3.9 \text{ min g}_{\text{cat}} \text{g}_{\text{reactant}}^{-1}$ , 580 mg reactant, 20.5 g C<sub>14</sub>H<sub>30</sub> solvent. The lines are included to guide the eye.

liquid solution. The model also indicates that, at 30 bar H<sub>2</sub> and 350 °C, 71% of the propylphenol is in the liquid phase (0.17 mmol g<sup>-1</sup>), and at 80 bar H<sub>2</sub> and 350 °C, the percentage is 76% (0.18 mmol g<sup>-1</sup>). The concentration of H<sub>2</sub> in the liquid phase at 350 °C should be 0.39 mmol g<sup>-1</sup> at 30 bar H<sub>2</sub> and 1.2 mmol g<sup>-1</sup> at 80 bar H<sub>2</sub>.

The effect of the increasing ratios of the concentrations of H<sub>2</sub> to 4-propylphenol at 20, 30, and 80 bar H<sub>2</sub> and 350 °C were determined experimentally. The reactions were allowed to attain full 4-propylphenol conversion. At the end of the experiments, the pressure had dropped, due to H<sub>2</sub> consumption in HDO, by 0.8 bar in the 20 bar experiment and by 2.1 bar in the 30 bar experiment. In the 80 bar experiment, the pressure rapidly dropped by 5 bar and H<sub>2</sub> was replenished in order to maintain the pressure. In total, H<sub>2</sub> had to be replenished three times to avoid a drop below 75 bar. The results are presented in Figure 4. The selectivity to propylbenzene fell with respect to pressure, whilst the selectivity to propylcyclohexane increased.

The VLE at the end of each experiment in the  $\tau_B$  series at 250 °C and 20 bar was also calculated. The results approximately represent the system at the end of the reaction, immediately before cooling. The results are shown in Figures S9 and S10 (Supporting Information). According to the VLE model, the concentration of H<sub>2</sub> in the liquid phase remained roughly constant at all residence times. Although the amount of alkylphenol decreased as it was consumed in the reaction, its distribution between the phases remained roughly constant, with ≈66% residing in the liquid phase. Furthermore, according to the model, 20% of the mass of the solvent evaporated, 60% of propylbenzene and 63% of propylcyclohexane remained in the liquid phase after being formed, and over 99.9% of the formed H<sub>2</sub>O evaporated.

Hydrogen concentration was higher than 4-propylphenol concentration in the liquid phase at all the tested pressures (Figure S8, Supporting Information) and batch residence times (Figure S10, Supporting Information). Nevertheless, deoxygenation and full hydrogenation to propylcyclohexane requires 4 mol of H<sub>2</sub> per mole of 4-propylphenol. The initial ratios of the molar amounts of H<sub>2</sub> and 4-propylphenol were <4 at 20 and 30 bar. At 20 bar, the H<sub>2</sub>:4-propylphenol ratio became >4 after 0.5 min  $\text{g}_{\text{cat}} \text{g}_{\text{reactant}}^{-1}$ , viz. at ≈70% 4-propylphenol conversion. At 80 bar, the initial H<sub>2</sub>:4-propylphenol ratio was ≈7. Thus, H<sub>2</sub> was the

limiting reactant to full hydrogenation at the tested conditions, except at 80 bar. Consequently, the limited amount of  $H_2$  in the liquid phase might have favored the low propylcyclohexane selectivity observed at the two lower pressures (Figure 4). This agrees with the observations of other authors,<sup>[16,26]</sup> who have pointed out the influence of  $H_2$  solubility on catalytic performance. From VLE calculations, it also appears that the distribution of the components across the phases remained roughly constant throughout  $\tau_B$  (Figure S9, Supporting Information). This suggests that the components were being transferred from one phase to the other as they were being consumed or produced.

## 2.6. Effects of Chemical Equilibrium, Temperature, and Pressure

The theoretical equilibrium compositions (Figure 5) were calculated for the present system with HSC Chemistry using the

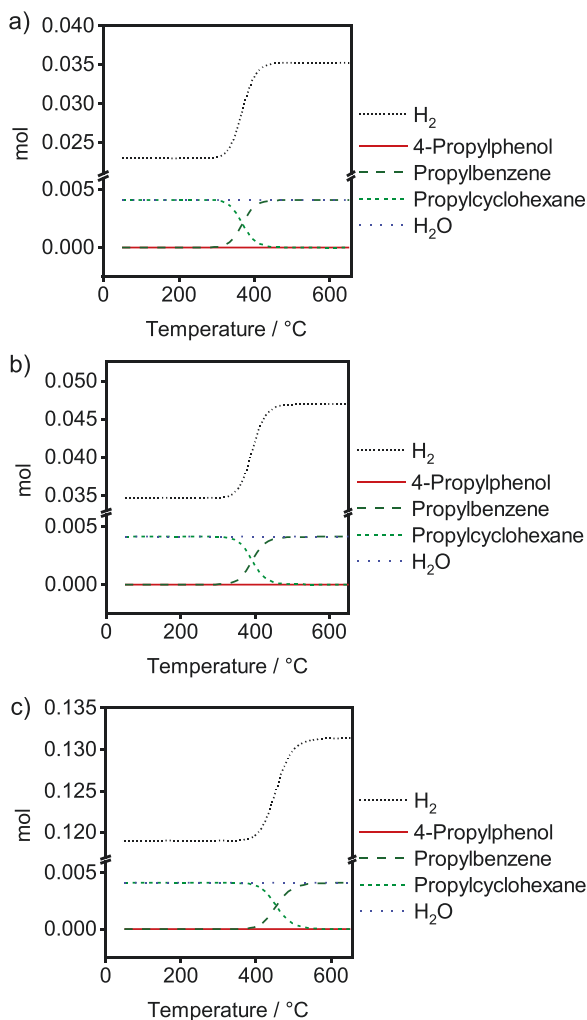


**Figure 5.** Temperature dependence of the theoretical chemical equilibrium composition of the H<sub>2</sub>O reaction mixture (excluding the solvent) at a) 20 bar H<sub>2</sub>, b) 30 bar H<sub>2</sub>, and c) 80 bar H<sub>2</sub>. The compositions were calculated in HSC Chemistry with initial amounts of 0.004 mol 4-propylphenol, 0 mol products, and a) 0.04 mol H<sub>2</sub>, b) 0.06 mol H<sub>2</sub>, and c) 0.14 mol H<sub>2</sub>. Note the scale breaks.

initial amounts of  $H_2$  and 4-propylphenol that were in the liquid phase, according to the VLE model. 4-Propylphenol should be fully consumed at equilibrium at all temperatures between 50 and 700 °C. At the lower temperatures, the amount of propylbenzene should be close to zero, whereas the amount of propylcyclohexane should be at its maximum. The positions of the two products should be inverted at the higher temperatures. The transitions should occur over a range of  $\approx 100$  °C. The curves of propylbenzene and propylcyclohexane intersect at their inflection points, indicating that the amounts of both species should be equal at a given temperature. This intersection temperature should increase with pressure; 370 °C at 20 bar, 390 °C at 30 bar, and 450 °C at 80 bar. The molar amount of  $H_2$  should be at its lowest where propylcyclohexane is at its highest. Furthermore, the amounts of  $H_2$  and propylbenzene should increase with temperature. The simulations included only the reactants, the two main products, and water. When propylcyclohexanone and propylcyclohexanol were included, their equilibrium molar amounts were 10 orders of magnitude below the main products throughout the temperature range.

The combined effects of temperature and pressure were tested experimentally. The reactor imposed an upper limit of  $\approx 410$  °C. Furthermore, in order to minimize the variation of 4-propylphenol concentration in the liquid phase resulting from VLE (Section 2.5), the temperatures had to be tested in two sets of experiments, each set with its own  $H_2$  pressure. At 20 bar, the initial 4-propylphenol concentration in the liquid phase was expected to be 0.18 mmol g<sup>-1</sup> at 300 °C and 0.16 mmol g<sup>-1</sup> at 350 °C, whereas at 30 bar, the expected initial concentration was 0.17 mmol g<sup>-1</sup> at 350 °C and 0.16 mmol g<sup>-1</sup> at 375 °C. The reactions were allowed to attain full 4-propylphenol conversion. The results are illustrated in Figure 6.

At 20 bar, propylbenzene was strongly disfavored at 300 °C and strongly favored at 350 °C. The opposite was true of propylcyclohexane. Similarly, at 30 bar, the preferred products were switched from 350 to 375 °C, with propylbenzene being more favored at 375 °C. The temperatures of the “inflection points” in the experimental results did not match the values predicted by the simulations (Figure 5), which were overestimated. An important source of this deviation is that the calculations neglected the non-ideal liquid behavior. Another cause of the mismatch could have been the uncertainty (9.9 kJ mol<sup>-1</sup>[59]) of the reported  $\Delta G_f^\circ$ [41] that was used in the calculations. However, a sensitivity analysis revealed no difference in the calculated equilibrium composition when  $\Delta G_f^\circ$  was varied within the uncertainty range. In any case, the trends reported by the theoretical calculations (Figure 5) were observed in the experiments (Figure 6); nearly full conversion of 4-propylphenol was attained and low amounts of oxygenates were formed in the experiments. Indeed, the liquid byproducts were benzenes and cyclopentanes in the four experiments, whereas oxygenated byproducts were only found at 300 °C. A high production of gases was observed at 375 °C, which did not occur at the lower temperatures.

It must be noted that, for the 30 bar experiments in Figure 6, the catalyst reduction temperature had to be higher (400 °C) than in all the other experiments (353 °C). The reason was that, at 30 bar, one experiment was performed at a higher temperature (375 °C) than the usual catalyst reduction temperature. In



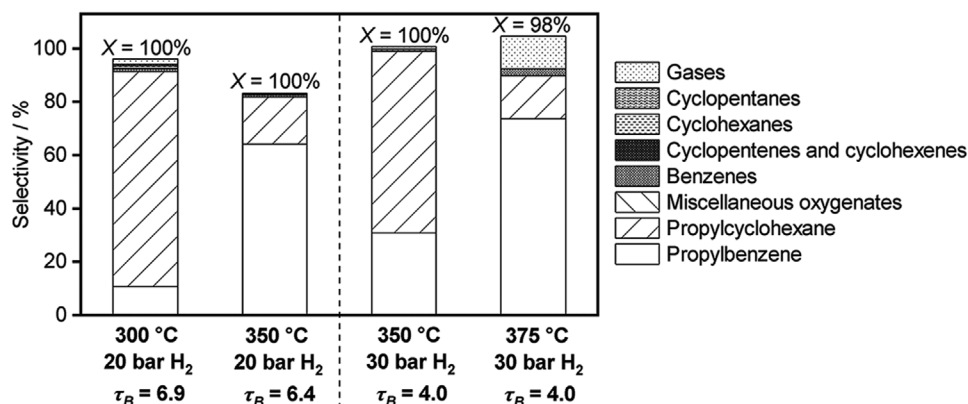


**Figure 6.** Effect of temperature and pressure on product selectivities at full conversion of 4-propylphenol (X). Batch residence times ( $\tau_B$ , min  $g_{cat} g_{reactant}^{-1}$ ) were adjusted to ensure full conversion at all the temperatures. Experiment parameters: 3.1%Pt/Nb<sub>2</sub>O<sub>5</sub> catalyst, 580 mg reactant, 20.5 g C<sub>14</sub>H<sub>30</sub> solvent. Catalyst reduction: 20 bar and 353 °C for the 20 bar H<sub>2</sub> experiments; 20 bar and 400 °C for the 30 bar H<sub>2</sub> experiments.

order to account for the influence of catalyst reduction temperature, HDO experiments were performed at equal conditions, varying only the catalyst reduction temperatures (Figure S12, Supporting Information). No differences were observed when HDO was performed at 20 bar and  $\approx 0.26$  min  $g_{cat} g_{reactant}^{-1}$  or at 30 bar and  $\approx 4$  min  $g_{cat} g_{reactant}^{-1}$ . However, at 20 bar and  $\approx 4$  min  $g_{cat} g_{reactant}^{-1}$ , the propylcyclohexane selectivity was 13% with 353 °C catalyst reduction and 50% with 400 °C catalyst reduction; this difference is difficult to explain. Nevertheless, it is more relevant that, at 30 bar, the catalyst reduction caused no difference in the HDO results. Because the catalysts reduced at the higher temperature were used only in the 30 bar experiments in Figure 6, it is likely that the catalyst reduction temperature did not influence the results presented in this work.

Figure S11 (Supporting Information) plots the chemical equilibrium constants calculated for temperatures between 0 and 1000 °C in the reactions of H<sub>2</sub> and 4-propylphenol to propylbenzene (Equation (6)) and to propylcyclohexane (Equation (7)). Propylbenzene hydrogenation (Equation (8)) and propylcyclohexane dehydrogenation (Equation (8), reverse) were also calculated. The equilibrium constants of propylbenzene formation are greater than the constants of propylcyclohexane formation at  $>250$  °C. Similarly, the constants of propylcyclohexane dehydrogenation are greater than the constants of propylbenzene hydrogenation at  $>250$  °C. The constants of the reactions of 4-propylphenol are greater at all temperatures than the reactions of propylbenzene and propylcyclohexane.

Thermodynamic and kinetic arguments have been used in the literature to explain the effects of temperature and pressure. Ruddy et al.<sup>[17]</sup> calculated the chemical equilibrium constants for the deoxygenation of cyclohexanone and phenol, and found them unfavorable above 400 °C. Furthermore, hydrogenation<sup>[44]</sup> and H<sub>2</sub> adsorption<sup>[62]</sup> are exothermic. A low amount of adsorbed H introduces kinetic limitations. Thus, at high temperature, hydrogenation can be both thermodynamically and kinetically limited. The high temperature in question depends on the specific reactant and catalyst; for example, Gutierrez et al.<sup>[62]</sup> identified guaiacol hydrogenation on Pt/ZrO<sub>2</sub> as kinetically hindered at 300 °C, but not thermodynamically. The activation energy of hydrogenation is lower than the activation energy of deoxygenation; hence, the former is favored kinetically at low

temperatures, whereas the rate of deoxygenation increases more rapidly with temperature, such that the ratio of hydrogenation to deoxygenation is inverted at higher temperatures.<sup>[17,63]</sup> The effect of H<sub>2</sub> pressure depends on the ability of the catalyst to activate H<sub>2</sub>; the more active the catalyst, the lesser the effect of H<sub>2</sub> pressure.<sup>[17]</sup>

In the present work, the selectivity to propylbenzene was favored, theoretically (Figure 5) and experimentally (Figure 6), when the pressure was lowered and when the temperature was raised. Thus, an interaction between the two variables was revealed. The VLE imposed limits to the possible combinations of temperature and pressure, as the presence of the reactant in the liquid phase was desired.

### 3. Conclusion

Aromatic hydrocarbons were obtained with high selectivity from propylphenols in HDO. A well-dispersed, highly active Pt/Nb<sub>2</sub>O<sub>5</sub> catalyst provided a propylbenzene selectivity of up to 77% from 4-propylphenol at 20 bar H<sub>2</sub>, 350 °C and 3.9 min  $g_{cat} g_{reactant}^{-1}$ . The main byproduct was propylcyclohexane, and nearly full deoxygenation was attained. *n*-Tetradecane was found to be advantageous to use as a solvent, whereas *n*-octane was found to be disadvantageous.

Certain factors were found to be detrimental to propylbenzene selectivity. Firstly, propylbenzene was consumed after being produced; propylbenzene selectivity decreased visibly after 5 min  $g_{cat} g_{reactant}^{-1}$ . Secondly, the position of the substituent in the parent alkylphenol influenced the selectivity to propylbenzene. In this study, 4-propylphenol was the most favorable for propylbenzene formation; and 2-propylphenol, the most unfavorable.

Some process parameters were advantageous to propylbenzene production. The low solubility of H<sub>2</sub> in the liquid reaction mixture at 20 bar allowed minimizing the production of propylcyclohexane in favor of propylbenzene. Furthermore, the chemical equilibrium should shift across a given temperature range from favoring propylcyclohexane to favoring propylbenzene. The precise temperature of such shift should depend on pressure. In this work, 350 °C was required to

favor propylbenzene at 20 bar, and 375 °C was required at 30 bar. The HDO of propylphenols was influenced by a complex combination of process parameters, which sometimes counteracted each other.

## 4. Experimental Section

**Materials:** The reagents used in this work were purchased from Sigma Aldrich and used without further purification. For HDO experiments, the reagents included 2-propylphenol (98%), 3-propylphenol (provided as a unique chemical without confirmation of identity or purity), 4-propylphenol (≥97%), *n*-octane (98%), and *n*-tetradecane (≥99%). The reagents used as calibration standards were propylbenzene (98%), propylcyclohexane (99%), and 2-isopropylphenol (98%), the latter being used as an internal standard (added to the GC vials with the product samples) and the former two, as external standards. The reagents that were used as solvents in experiments, *n*-octane and *n*-tetradecane, were measured for sulfur content with the ASTM D7039 MWD XRF method. The measured values were below the detection limit of the method (0.15 ppm).

The gases were purchased from Oy AGA AB. H<sub>2</sub> (purity 5.0) was used both in HDO experiments and for analytical techniques. The analytical techniques also required He (purity 4.6), Ar (purity 5.0), synthetic air (purity 5.0), and N<sub>2</sub> (purity 5.0). Two calibration gas mixtures were used. The first contained 40 mol% N<sub>2</sub>, 5 mol% CH<sub>4</sub>, 10 mol% ethane, 5 mol% ethane, 10 mol% propane, 5 mol% propene, 5 mol% acetylene, 10 mol% butane, and 10 mol% isobutene. The second calibration mixture contained 15 vol% CO, 15 vol% CO<sub>2</sub>, 15 vol% H<sub>2</sub>, 40 vol% N<sub>2</sub> and 15 vol% CH<sub>4</sub>.

The niobium oxide hydrate used to prepare the catalyst support was provided by Companhia Brasileira de Metalurgia e Mineração (CBMM), whilst the metal precursor, Pt(NO<sub>3</sub>)<sub>4</sub> solution (15% w/w Pt) was purchased from Alfa Aesar.

**Catalyst Preparation and Characterization:** The 3% Pt/Nb<sub>2</sub>O<sub>5</sub> catalyst was prepared by incipient wetness impregnation using appropriate amount of metal precursor solution, determined by approximating the support pore volume from its capacity to uptake water. Before the impregnation, the niobium oxide hydrate powder was thermally treated at a moderate temperature (270 °C) to increase the strength of the pressed tablets, which were ground to 0.25–0.42 mm particle size. Final calcination of the support particles was conducted at 500 °C for 7 h under 100 mL min<sup>−1</sup> synthetic air flow. The final calcination temperature used was typical for Nb<sub>2</sub>O<sub>5</sub> support,<sup>[64,65]</sup> since it transforms the amorphous niobic acid into pseudo-hexagonal TT–Nb<sub>2</sub>O<sub>5</sub>.<sup>[34]</sup> The TT–Nb<sub>2</sub>O<sub>5</sub> typically has a high surface area, which is preferred for a catalyst support.<sup>[66]</sup> After impregnation, the catalyst was dried at room temperature for 5 h and then overnight at 100 °C and thermally treated at 350 °C for 3 h with 100 mL min<sup>−1</sup> synthetic air flow, which was similar to the procedures presented in the literature.<sup>[32,64]</sup> The actual metal loading of the catalyst was determined by X-ray fluorescence (XRF) using a PANalytical Axios Max wavelength dispersive spectrometer with an X-ray source of SST-max. The catalyst was characterized further using N<sub>2</sub> physisorption, CO chemisorption, and scanning transmission electron microscopy (STEM). The detailed methodology is reported in Section S1 (Supporting Information).

**HDO Experiments and Product Analysis:** HDO experiments were performed in a 100 mL Parr batch autoclave. The reactions proceeded with *n*-tetradecane as a solvent and with the catalyst in slurry with the liquid phase. Before each experiment, the catalyst was weighed, placed in the reactor, and dried at 180 °C for 1 h in 10 bar N<sub>2</sub>. Depending on the desired batch residence time, the amount of catalyst was 10, 16, 32, or 65 mg. After drying, the hot N<sub>2</sub> was vented and the reactor was cooled down to 30 °C with a water bath and ice. Next, the reactor was flushed and pressurized with 10 bar H<sub>2</sub>, and it was heated up to 353 °C for reduction, while stirring at 200 rpm. Once the reduction temperature was attained, the H<sub>2</sub> was vented and the reactor was pressurized again to 20 bar with fresh H<sub>2</sub>. After 1 h reduction, the reactor was cooled down

to room temperature. For HDO, the reactor was vented to atmospheric pressure, although the H<sub>2</sub> atmosphere was kept, and heated up to the desired reaction temperature (300, 350, or 375 °C). When the reaction temperature was attained, a mixture of 580 mg propylphenol in 27 mL (≈20.5 g) *n*-tetradecane was injected from the feed vessel of the reactor, the reactor was pressurized with pure H<sub>2</sub> (20, 30, or 80 bar), and stirring at 645 rpm was started. The reaction time was counted from the time of pressurization. At the end of this time, the furnace was removed and the reactor was allowed to cool down to 200 °C. Then, a water bath was applied to accelerate cooling and, from 50 °C, ice was used. The gas phase was sampled at ≈20 °C, when the reactor was stable and the pressure was 10–15 bar. The exact temperatures and pressures at the time of sampling were recorded. Finally, the reactor was vented and the liquid products were recovered along with the spent catalyst.

The ratio of reaction time and amount of catalyst to the amount of reactant is defined in this work as batch residence time ( $\tau_B$ , Equation (1)).<sup>[67,68]</sup> This concept is used instead of reaction time to report the results, because both the reaction time and the catalyst amount had to be modified in order to attain different levels of conversion. Furthermore, conversion time series are insufficient to represent catalytic activity, hence it has been recommended<sup>[69,70]</sup> to report the duration of the reaction in relative values that correct for some of the specific parameters used. The values used to calculate  $\tau_B$  for each experiment are reported in Table S1 (Supporting Information).

After the reaction, the gas sample was analyzed in an Agilent 6890 series GC analyzer equipped with HP-AL/KCL, HP-PLOT/Q, and HP Molesieve columns. The products in the organic phase were identified with an Agilent GC-MS 7890-5975 and quantified with an HP 6890 Series GC-FID. Both GC systems used a Zebron ZB-wax Plus column. Finally, the water content in the organic phase was determined with Karl-Fischer titration (SI Analytics TitroLine 7500 KF); no more water was detected in the HDO products than in the fresh solvent. Further details are given in Section S2 (Supporting Information).

**Calculations:** Batch residence time ( $\tau_B$ , min g<sub>cat</sub> g<sub>reactant</sub><sup>−1</sup>) is defined in this work as

$$\tau_B = \frac{m_{\text{cat}}}{m_A} t \quad (1)$$

where  $m_{\text{cat}}$  is the mass of catalyst (g),  $m_A$  is the initial mass of reactant (g), and  $t$  is the reaction time (min). Conversions, selectivities, and yields were calculated from the concentrations of the reactant and the products obtained from GC analysis. Conversion ( $X$ ) is defined as

$$X = \frac{n_{A,0} - n_{A,f}}{n_{A,0}} \quad (2)$$

where  $n_{A,0}$  is the molar amount of reactant at the beginning of the experiment and  $n_{A,f}$  is the molar amount of reactant at the end. The selectivity to product  $i$  ( $S_i$ ) is defined as

$$S_i = \frac{|v_A| n_{P,i}}{v_P (n_{A,0} - n_{A,f})} \quad (3)$$

where  $n_{P,i}$  is the molar amount of product obtained in the experiment,  $v_A$  is the stoichiometric factor of the reactant, and  $v_{P,i}$  is the stoichiometric factor of product  $i$ . The mass-based selectivity was calculated analogously to Equation (3), except that the stoichiometric factors were excluded. The estimation of the stoichiometric factors, as well as the calculations of the amounts of initial H<sub>2</sub> and final gases, and of the initial turnover frequencies (TOF<sub>0</sub>, s<sup>−1</sup>), are explained in Section S8 (Supporting Information).

The sum of moles of carbon present in the recovered, quantified products and unconverted reactant with respect to the carbon moles present in the initial propylphenol reactant constitute the carbon balance

$$B_C = \frac{N_{C,A} n_{A,f} + \sum_i N_{C,P,i} n_{P,i}}{N_{C,A} n_{A,0}} \quad (4)$$

Equation (4) excludes the solvent and its cracking products. The cases where the carbon balances added >100% can be explained by uncertainties in the calculation of the stoichiometric factors (Equation S13, Supporting Information). The mass balances are the ratio of the overall quantified masses of gas, liquid, and solid recovered after the experiments with respect to the total mass of reactant, solvent, and catalyst added to the reactor. Furthermore, the sums of mass-based selectivities per experiment ( $\Sigma Sm$ ) indicate the closure of the mass balances of the products with respect to the initial reactant, excluding solvent and catalyst

$$100\% = \frac{\sum_i m_{P,i}}{m_{A,0} - m_{A,f}} + \frac{\text{loss}}{m_{A,0} - m_{A,f}} = \Sigma Sm + \text{loss}\% \quad (5)$$

The carbon and mass balances and  $\Sigma Sm$  of the conducted experiments are reported in Table S3 (Supporting Information).

**Computer Models:** Calculations with the PSRK method were performed in Aspen Plus<sup>[71]</sup> version 8.8 for the VLE of HDO. Propylphenols were not available in Aspen's database. Hence, the physical properties of propylphenols were retrieved from the literature<sup>[41]</sup> and inputted to the program. The retrieved values are reported in Table S4 (Supporting Information). Further inputs were the amounts of H<sub>2</sub>, C<sub>14</sub>H<sub>30</sub>, 4-propylphenol, propylbenzene, propylcyclohexane, and H<sub>2</sub>O that were either fed to the reactor before the experiments or quantified afterward. The EoS was solved for a series of temperatures (300–375 °C) and pressures (20–80 bar) with the initial mixture of H<sub>2</sub>, C<sub>14</sub>H<sub>30</sub>, and 4-propylphenol. The simulations were also run to determine the VLE of the reaction mixture at the different points of  $\tau_B$  corresponding to the performed experiments.

The chemical equilibria of the HDO reactions were calculated with the Gibbs energy minimization method using HSC Chemistry software version 6.<sup>[72]</sup> The equilibrium constants of the following overall reactions were calculated



where C<sub>9</sub>H<sub>12</sub>O is 4-propylphenol, C<sub>9</sub>H<sub>12</sub> is propylbenzene, and C<sub>9</sub>H<sub>18</sub> is propylcyclohexane. Furthermore, the chemical equilibrium compositions of a reaction system comprising H<sub>2</sub>, 4-propylphenol, propylbenzene, propylcyclohexane, and water were computed based on the total initial amounts of H<sub>2</sub> and 4-propylphenol in the reactor. The equilibrium compositions at 20, 30, and 80 bar were determined in the range of 50 to 700 °C. Propylphenols were not available in the database of HSC Chemistry. Therefore, the required properties, retrieved from the literature<sup>[41]</sup> and reported in Table S4 (Supporting Information), were inputted.

## Supporting Information

Supporting Information is available from the Wiley Online Library or from the author.

## Acknowledgements

This work was funded mainly by Neste Corporation. J.L.G.E. acknowledges a personal grant (no. 201800142) from Fortum Foundation and from the Finnish Foundation for Technology Promotion (no. 6712). E.M. acknowledges a grant from Aalto University.

Heidi Meriö-Talvio from Aalto University is thanked for help with the identification of 1-methoxy-4-(1-methylpropyl)-benzene. Dr. Jaana Kanervo from Neste Engineering Solutions and Dr. Aitor Arandia

Gutiérrez from Aalto University are thanked for valuable comments to the manuscript. The authors acknowledge Companhia Brasileira de Metalurgia e Mineração (CBMM) for providing the niobium oxide hydrate. Dr. Hua Jiang is thanked for producing the STEM images at Aalto University's OtaNano–Nanoscience Center (Aalto-NMC). The Finnish national BioEconomy infrastructure and Raw Materials Research Infrastructure (RAMI) are acknowledged for equipment support.

## Conflict of Interest

The authors declare no conflict of interest.

## Keywords

hydrodeoxygenation, niobia, platinum, process parameters, propylphenols

Received: December 4, 2019

Revised: February 28, 2020

Published online: April 27, 2020

- [1] K. Van Meerbeek, B. Muys, M. Hermy, *Renewable Sustainable Energy Rev.* **2019**, *102*, 139.
- [2] M. Triviño, A. Juutinen, A. Mazziotto, K. Miettinen, D. Podkopaev, P. Reunanen, M. Mönkkönen, *Ecosyst. Serv.* **2015**, *14*, 179.
- [3] O. Boiral, I. Heras-Saizarbitoria, *Environ. Sci. Policy* **2017**, *77*, 77.
- [4] H. Wei, W. Liu, X. Chen, Q. Yang, J. Li, H. Chen, *Fuel* **2019**, *254*, 115599.
- [5] M. Fatih Demirbas, *Appl. Energy* **2009**, *86*, S151.
- [6] J. P. Lange, *ChemSusChem* **2018**, *11*, 997.
- [7] M. R. Haverly, T. C. Schulz, L. E. Whitmer, A. J. Friend, J. M. Funkhouser, R. G. Smith, M. K. Young, R. C. Brown, *Fuel* **2018**, *211*, 291.
- [8] H. Wang, J. Male, Y. Wang, *ACS Catal.* **2013**, *3*, 1047.
- [9] R. Schmidt, K. Griesbaum, A. Behr, D. Biedenkapp, H.-W. Voges, D. Garbe, C. Paetz, G. Collin, D. Mayer, H. Höke, *Ullmann's Encyclopedia of Industrial Chemistry*, Wiley-VCH Verlag GmbH & Co. KGaA, Weinheim, Germany **2014**, pp. 1–74.
- [10] J. Fabri, U. Graeser, T. A. Simo, in *Ullmann's Encyclopedia of Industrial Chemistry*, Vol. 39, Wiley-VCH Verlag GmbH & Co. KGaA, Weinheim, Germany **2000**, pp. 643–663.
- [11] V. A. Welch, K. J. Fallon, H.-P. Gelbke, in *Ullmann's Encyclopedia of Industrial Chemistry*, Vol. 13, Wiley-VCH Verlag GmbH & Co. KGaA, Weinheim, Germany **2005**, pp. 451–464.
- [12] J. Fabri, U. Graeser, T. A. Simo, in *Ullmann's Encyclopedia of Industrial Chemistry*, Wiley-VCH Verlag GmbH & Co. KGaA, Weinheim, Germany **2011**, pp. 109–118.
- [13] L. Collier, C. Viljoen, M. Ajam, M. Ndlovu, D. Yoell, P. Gravett, N. Esterhuysen, in *Significance of Tests for Petroleum Products* (Ed: S. J. Rand), ASTM International, West Conshohocken, PA **2010**, pp. 304–315.
- [14] K. Strauss, in *Significance of Tests for Petroleum Products* (Ed: S. J. Rand), ASTM International, West Conshohocken, PA **2003**, pp. 89–101.
- [15] M. Hellinger, H. W. P. de Carvalho, S. Baier, L. Gharnati, J.-D. Grunwaldt, *Chem. Ing. Tech.* **2015**, *87*, 1771.
- [16] J. He, C. Zhao, J. A. Lercher, *J. Catal.* **2014**, *309*, 362.
- [17] D. A. Ruddy, J. A. Schaidle, J. R. Ferrell III, J. Wang, L. Moens, J. E. Hensley, *Green Chem.* **2014**, *16*, 454.
- [18] F. E. Massoth, P. Politzer, M. C. Concha, J. S. Murray, J. Jakowski, J. Simons, *J. Phys. Chem. B* **2006**, *110*, 14283.
- [19] E. Laurent, B. Delmon, *Ind. Eng. Chem. Res.* **1993**, *32*, 2516.

- [20] B. Pawelec, J. L. García Fierro, in *Catalytic Hydrogenation for Biomass Valorization* (Ed: R. Rinaldi), The Royal Society Of Chemistry, Cambridge, UK **2015**, pp. 174–203.
- [21] W. Wang, S. Tan, K. Wu, G. Zhu, Y. Liu, L. Tan, Y. Huang, Y. Yang, *Fuel* **2018**, 214, 480.
- [22] H. Ohta, B. Feng, H. Kobayashi, K. Hara, A. Fukuoka, *Catal. Today* **2014**, 234, 139.
- [23] M. B. Griffin, G. A. Ferguson, D. A. Ruddy, M. J. Biddy, G. T. Beckham, J. A. Schaidle, *ACS Catal.* **2016**, 6, 2715.
- [24] Q. Tan, G. Wang, L. Nie, A. Dinse, C. Buda, J. Shabaker, D. E. Resasco, *ACS Catal.* **2015**, 5, 6271.
- [25] A. J. Foster, P. T. M. Do, R. F. Lobo, *Top. Catal.* **2012**, 55, 118.
- [26] H. Wan, R. V. Chaudhari, B. Subramaniam, *Top. Catal.* **2012**, 55, 129.
- [27] G. H. Gu, C. A. Mullen, A. A. Boateng, D. G. Vlachos, *ACS Catal.* **2016**, 6, 3047.
- [28] A. M. Robinson, J. E. Hensley, J. Will Medlin, *ACS Catal.* **2016**, 6, 5026.
- [29] P. M. de Souza, R. C. Rabelo-Neto, L. E. P. Borges, G. Jacobs, B. H. Davis, T. Sooknoi, D. E. Resasco, F. B. Noronha, *ACS Catal.* **2015**, 5, 1318.
- [30] L. Nie, D. E. Resasco, *J. Catal.* **2014**, 317, 22.
- [31] P. M. de Souza, R. C. Rabelo-Neto, L. E. P. Borges, G. Jacobs, B. H. Davis, D. E. Resasco, F. B. Noronha, *ACS Catal.* **2017**, 7, 2058.
- [32] A. M. Barrios, C. A. Teles, P. M. de Souza, R. C. Rabelo-Neto, G. Jacobs, B. H. Davis, L. E. P. Borges, F. B. Noronha, *Catal. Today* **2018**, 302, 115.
- [33] C. A. Teles, P. M. de Souza, R. C. Rabelo-Neto, M. B. Griffin, C. Mukarakate, K. A. Orton, D. E. Resasco, F. B. Noronha, *Appl. Catal., B* **2018**, 238, 38.
- [34] I. Nowak, M. Ziolek, *Chem. Rev.* **1999**, 99, 3603.
- [35] C. Hernández Mejía, J. H. den Otter, J. L. Weber, K. P. de Jong, *Appl. Catal., A* **2017**, 548, 143.
- [36] Q. Xia, Z. Chen, Y. Shao, X. Gong, H. Wang, X. Liu, S. F. Parker, X. Han, S. Yang, Y. Wang, *Nat. Commun.* **2016**, 7, 11162.
- [37] H. Pourzolfaghari, F. Abnisa, W. M. A. Wan Daud, M. K. Aroua, *J. Anal. Appl. Pyrolysis* **2018**, 133, 117.
- [38] U. K. Singh, M. A. Vannice, *Appl. Catal., A* **2001**, 213, 1.
- [39] R. C. Nelson, B. Baek, P. Ruiz, B. Goundie, A. Brooks, M. C. Wheeler, B. G. Frederick, L. C. Grabow, R. N. Austin, *ACS Catal.* **2015**, 5, 6509.
- [40] E. M. Turpeinen, E. Sapei, P. Uusi-Kyyny, K. I. Keskinen, O. A. I. Krause, *Fuel* **2011**, 90, 3315.
- [41] C. L. Yaws, *Yaws' Handbook of Thermodynamic Properties for Hydrocarbons and Chemicals*, Knovel, Norwich, New York **2014**.
- [42] M. L. Michelsen, *Fluid Phase Equilib.* **1996**, 121, 15.
- [43] H. Shafaghhat, P. S. Rezaei, W. M. Ashri Wan Daud, *RSC Adv.* **2015**, 5, 103999.
- [44] X. Zhang, J. Tang, Q. Zhang, Q. Liu, Y. Li, L. Chen, C. Wang, L. Ma, *Catal. Today* **2019**, 319, 41.
- [45] S. C. Lee, S. W. Lee, K. S. Kim, T. J. Lee, D. H. Kim, J. C. Kim, *Catal. Today* **1998**, 44, 253.
- [46] A. M. Scheer, C. Mukarakate, D. J. Robichaud, M. R. Nimlos, H. H. Carstensen, G. Barney Ellison, *J. Chem. Phys.* **2012**, 136, 044309.
- [47] T. R. Viljava, R. S. Komulainen, A. O. I. Krause, *Catal. Today* **2000**, 60, 83.
- [48] B. Yoosuk, D. Tumnantong, P. Prasassarakich, *Chem. Eng. Sci.* **2012**, 79, 1.
- [49] S. D. Lin, M. A. Vannice, *J. Catal.* **1993**, 143, 563.
- [50] J. W. Thybaut, M. Saeys, G. B. Marin, *Chem. Eng. J.* **2002**, 90, 117.
- [51] P. Castaño, J. M. Arandes, B. Pawelec, J. L. G. Fierro, A. Gutiérrez, J. Bilbao, *Ind. Eng. Chem. Res.* **2007**, 46, 7417.
- [52] K. Ahmed, H. M. Chowdhury, *Chem. Eng. J.* **1992**, 50, 165.
- [53] J. P. Du, C. Song, J. L. Song, J. H. Zhao, Z. P. Zhu, *J. Fuel Chem. Technol.* **2009**, 37, 468.
- [54] A. A. Shukla, P. V. Gosavi, J. V. Pande, V. P. Kumar, K. V. R. Chary, R. B. Biniwale, *Int. J. Hydrogen Energy* **2010**, 35, 4020.
- [55] O. Saber, H. M. Gobara, *Egypt. J. Pet.* **2014**, 23, 445.
- [56] H. Du, C. Fairbridge, H. Yang, Z. Ring, *Appl. Catal., A* **2005**, 294, 1.
- [57] V. Calemme, A. Carati, C. Flego, R. Giardino, F. Gagliardi, R. Millini, G. Bellussi, *ChemSusChem* **2008**, 1, 548.
- [58] Q. Sun, G. Chen, H. Wang, X. Liu, J. Han, Q. Ge, X. Zhu, *ChemCatChem* **2016**, 8, 551.
- [59] R. C. Reid, J. M. Prausnitz, B. E. Poling, *The Properties of Gases and Liquids*, McGraw-Hill, USA **1987**, pp. 2.3–2.4, 3.6–3.8.
- [60] H. Weigold, *Fuel* **1982**, 61, 1021.
- [61] S. B. Gevert, M. Eriksson, P. Eriksson, F. E. Massoth, *Appl. Catal., A* **1994**, 117, 151.
- [62] A. Gutierrez, R. K. Kaila, M. L. Honkela, R. Slioor, A. O. I. Krause, *Catal. Today* **2009**, 147, 239.
- [63] M. Saidi, P. Rostami, H. R. Rahimpour, M. A. Roshanfekr Fallah, M. R. Rahimpour, B. C. Gates, S. Raeissi, *Energy Fuels* **2015**, 29, 4990.
- [64] K. Kon, W. Onodera, S. Takakusagi, K. I. Shimizu, *Catal. Sci. Technol.* **2014**, 4, 3705.
- [65] M. V. Cagnoli, A. M. Alvarez, N. G. Gallegos, J. F. Bengoa, C. D. D. de Souza, M. Schmal, S. G. Marchetti, *Appl. Catal., A* **2007**, 326, 113.
- [66] S. Li, Q. Xu, E. Uchaker, X. Cao, G. Cao, *CrystEngComm* **2016**, 18, 2532.
- [67] H. S. Fogler, *Elements of Chemical Reaction Engineering*, Pearson Education, Inc., Westford, Massachusetts, USA **2006**, pp. 66–67.
- [68] F. Kapteijn, J. Gascon, T. A. Nijhuis, in *Catalysis: An Integrated Textbook for Students* (Eds: U. Hanefeld, L. Lefferts), Wiley-VCH Verlag GmbH & Co., Weinheim, Germany **2008**, pp. 221–271.
- [69] M. Boudart, *Chem. Rev.* **1995**, 95, 661.
- [70] O. Deutschmann, H. Knözinger, K. Kochloeff, T. Turek, in *Ullmann's Encyclopedia of Industrial Chemistry*, Vol. 17, Wiley-VCH Verlag GmbH & Co. KGaA, Weinheim, Germany **2011**, pp. 457–481.
- [71] Aspen Technology Inc., Aspen Plus v8.8 software, USA, **1981**.
- [72] T. Kotiranta, R. Ahlberg, A. Gröhn, A. Roine, P. Lamberg, J. Mansikka-aho, *HSC Chemistry version 6.12 software*, Outotec Research Oy, Pori, Finland **2007**.